Vibrational assignment and absolute integrated intensities of liquid bromobenzene-d5 between 4000 and 400 cm−1 at 25 °C

ARTICLE *in* JOURNAL OF MOLECULAR STRUCTURE · SEPTEMBER 2005

Impact Factor: 1.6 · DOI: 10.1016/j.molstruc.2005.05.019

2 AUTHORS:

Dale Keefe
Cape Breton University
54 PUBLICATIONS **721** CITATIONS
SEE PROFILE

Jason K Pearson
University of Prince Edward Island
28 PUBLICATIONS **240** CITATIONS
SEE PROFILE

Available online at www.sciencedirect.com
SCIENCE DIRECT
Journal of Molecular Structure 751 (2005) 190–199
Journal of MOLECULAR STRUCTURE
www.elsevier.com/locate/molstruc

Vibrational assignment and absolute integrated intensities of liquid bromobenzene-d_5 between 4000 and 400 cm^{-1} at 25 °C

C. Dale Keefe*, Jason K. Pearson

Department of Physical and Applied Sciences, Cape Breton University, Sydney, Nova Scotia, Canada, B1P 6L2

Received 13 December 2004; revised 11 May 2005; accepted 11 May 2005
Available online 1 July 2005

Abstract

This paper continues the analysis of the integrated intensities of substituted benzenes. In particular, the absolute integrated vibrational intensities of bromobenzene-d_5 are presented. The previously reported imaginary molar polarizability spectrum of bromobenzene-d_5 was fitted with 231 CDHO bands. The majority of the bands are assigned to fundamentals, first overtones or binary combinations (sum and difference). From the fitted parameters, the integrated intensities of the fundamentals have been determined. Using the F-Sum rule, the intensities are compared to those of bromobenzene-h_5. The intensities agreed very well between the two isotopomers.

Keywords: Vibrational assignment; Liquid; Bromobenzene-d_5; Dipole moment derivatives; Integrated intensities

1. Introduction

Interest in the vibrational properties of benzene dates back to the 1930s with the work of Wilson [1]. Over the last decade, this laboratory has been involved in the exploration of the absolute infrared vibrational intensities of benzene and benzene derivatives in the liquid phase. The focus of this project is to understand how the intermolecular interactions in the liquid affect the vibrational intensities.

The integrated intensities in the liquid phase are obtained from the imaginary molar polarizability spectrum, which is determined from the complex refractive index spectra across the infrared. For a review of how one obtains complex refractive index spectra and the conversion to the imaginary molar polarizability spectrum, the reader is referred to Ref. [2] and references cited therein. Once the imaginary molar polarizability spectrum is known, the integrated intensities of the various transitions need to be determined. This is done by fitting the imaginary molar polarizability spectrum to a standard lineshape. The preferred [2–4] lineshape for the imaginary molar polarizability spectrum is the Classical Damped Harmonic Oscillator (CDHO) lineshape. From the integrated intensities, the transition moments and dipole moment derivatives can be obtained. It is these quantities that are compared between the different benzene compounds to gain insight into how the liquid phase vibrational intensities are dependent on the intermolecular interactions.

To date, the complex refractive index spectra, imaginary molar polarizability spectra, transition moments and dipole moment derivatives have been reported for benzene [5–7], benzene-d_6 [8], benzene-d_1 [9], and bromobenzene [10,11]. In addition, the complex refractive index spectra and imaginary molar polarizability spectra of bromobenzene-d_5 [12], hexafluorobenzene [13], ethylbenzene [14], fluorobenzene [15], toluene [16] and toluene-d_8 [17] have been reported. Work is presently underway to fit the imaginary molar polarizability spectra of these compounds.

In this paper, the fitting of the imaginary molar polarizability spectrum of bromobenzene-d_5 is reported. The imaginary molar polarizability spectrum [12] was fitted between 4000 and 400 cm^{-1}. Most of the required peaks were due to observable features within the spectrum and the assignments of most of the features in the infrared spectrum of liquid bromobenzene-d_5 are reported for the first time.

* Corresponding author. Tel.: +1 902 563 1185; fax: +1 902 563 1880.
E-mail address: dale_keefe@capebretonu.ca (C.D. Keefe).

0022-2860/$ - see front matter © 2005 Elsevier B.V. All rights reserved.
doi:10.1016/j.molstruc.2005.05.019

Table 1
Observed and fitted bands in the imaginary molar polarizability spectrum of liquid bromobenzene-d_5

Assignment[a]	obsd $\tilde{\nu}$[b]	Fitted band			Sum of C_j[d]
		$\tilde{\nu}_j$[c]	Γ_j[c]	C_j[d]	
		3954.6	84.7	62.4	
	3905 VW	3908.0	46.4	101.3	
	3890 VW	3887.9	20.6	25.6	
$\nu_4+\nu_{21}$	3841 Sh VW	3842.7	25.1	158.3	
$\nu_2+\nu_4$, $\nu_{21}+\nu_{23}$, $\nu_4+\nu_{22}$	3830 Sh VW	3833.4	6.0	11.8	
	3828 Sh VW	3828.5	10.6	46.5	
		3823.5	7.0	13.2	
$\nu_3+\nu_4$, $\nu_{22}+\nu_{23}$	3818 VW	3818.1	13.1	172.9	
$\nu_3+\nu_{23}$	3807 Sh VW	3808.2	10.4	63.7	
		3804.4	3.7	3.5	
	3795 VW	3795.8	12.3	165.8	
	3760 VW	3758.9	19.9	20.1	
	3738 VW	3737.6	13.0	18.0	
		3697.6	32.5	56.3	
	3682 VW	3681.6	23.1	102.6	
		3662.2	30.0	27.5	
		3637.1	19.2	29.2	
$\nu_5+\nu_{21}$	3630 VW	3631.3	8.8	14.5	
$\nu_1+\nu_{24}$, $\nu_2+\nu_5$	3620 VW	3621.4	12.2	60.7	
$\nu_5+\nu_{22}$	3618 Sh VW	3616.6	8.3	7.4	
$\nu_{21}+\nu_{24}$, $\nu_3+\nu_5$	3606 VW	3606.6	13.5	75.5	
$\nu_2+\nu_{24}$	3597 Sh VW	3597.0	16.8	43.8	
$\nu_3+\nu_{24}$, $\nu_1+\nu_{25}$, $\nu_{22}+\nu_{24}$	3584 Sh VW	3585.5	18.1	21.7	
$\nu_2+\nu_{25}$	3567 Sh VW	3566.9	24.3	30.8	
$\nu_3+\nu_{25}$	3548 VW	3548.8	17.8	78.4	
	3518 VW	I			
	3515 Sh VW	3515.6	35.5	31.4	
	3488 VW	I			
	3463 VW	3463.8	50.9	26.6	
	3412 VW	3414.0	39.3	19.9	
	3393 VW	3394.5	11.6	12.4	
	3378 VW	3377.6	14.9	17.1	
		3356.1	29.4	20.2	
	3337 Sh VW	3338.6	1.4	0.2	
	3334	3335.6	13.7	12.6	
$\nu_1+\nu_{26}$		3325.0	9.0	6.0	
$\nu_1+\nu_6$	3317 Sh VW	3317.9	11.4	17.5	
$\nu_{21}+\nu_{26}$		3311.1	11.4	28.5	
$\nu_6+\nu_{21}$	3303 Sh VW	3305.8	11.7	48.6	
$\nu_2+\nu_6$, $\nu_{22}+\nu_{26}$		3297.4	12.3	125.8	
$\nu_6+\nu_{22}$, $\nu_3+\nu_{26}$	3291 VW	3290.2	18.4	444.9	
$\nu_3+\nu_6$	3276 Sh VW	3277.7	17.0	38.2	
$\nu_2+\nu_7$		3240.9	11.5	128.0	
$\nu_7+\nu_{22}$	3233 W	3233.5	10.9	624.2	
$\nu_3+\nu_7$	3222 Sh VW	3221.3	6.7	37.4	
	3215 Sh VW	3214.8	9.7	89.8	
$\nu_1+\nu_8$		3167.3	41.7	50.6	
$\nu_2+\nu_8$, $\nu_1+\nu_{27}$	3146 VW	3147.0	14.3	75.2	
$\nu_2+\nu_{27}$, $\nu_1+\nu_9$, $\nu_1+\nu_{28}$	3123 Sh VW	3126.4	18.9	73.3	
$\nu_9+\nu_{21}$, $\nu_{21}+\nu_{28}$, $\nu_3+\nu_{27}$	3111 Sh VW	3112.0	14.8	100.7	
$\nu_2+\nu_{15}$		3103.1	9.2	47.4	
$\nu_2+\nu_9$, $2\nu_4$, $\nu_2+\nu_{28}$	3100 Sh VW	3099.5	7.2	28.2	
$\nu_{22}+\nu_{28}$	3097 Sh VW	3096.6	5.5	17.0	
$\nu_9+\nu_{22}$		3093.7	6.3	24.8	
$\nu_4+\nu_{23}$		3090.5	6.5	35.3	
$\nu_3+\nu_{28}$, $\nu_3+\nu_{15}$	3089 VW	3087.4	6.2	29.3	
$\nu_3+\nu_9$	3083 Sh VW	3084.2	6.4	24.3	
	3080 Sh VW	3080.8	7.1	21.0	
$2\nu_{23}$	3075 VW	3076.3	7.3	25.1	
	3072 Sh VW	3072.7	9.3	29.7	

(*continued on next page*)

Table 1 (*continued*)

Assignment[a]	obsd $\tilde{\nu}$[b]	Fitted band			Sum of C_j[d]
		$\tilde{\nu}_j$[c]	Γ_j[c]	C_j[d]	
	3066 Sh VW	3066.7	11.6	19.3	
$\nu_{12}+\nu_{21}$	3053 VW	3056.9	11.9	29.2	
$\nu_1+\nu_{16}$	3051 VW	3050.3	10.4	27.1	
	3044 Sh VW	3044.5	11.2	17.8	
$\nu_{12}+\nu_{22}$	3035 VW	3034.3	11.6	14.1	
$\nu_2+\nu_{16}$		3024.3	9.8	8.5	
	3018 VW	3017.9	9.4	12.1	
$\nu_3+\nu_{16}$	3011 Sh VW	3009.7	10.0	10.1	
	2963 Sh VW	2962.6	16.8	132.0	
$\nu_1+\nu_{10}$, $\nu_{13}+\nu_{22}$	2950 VW	2952.1	20.3	303.4	
$\nu_2+\nu_{10}$	2925 W	2925.3	22.2	1115.9	
$\nu_3+\nu_{10}$	2910 Sh VW	2909.8	18.7	177.0	
	2901 VW	2900.9	11.1	158.0	
$\nu_4+\nu_5$, $\nu_1+\nu_{29}$	2892 Sh VW	2894.0	10.7	71.8	
	2888 Sh VW	2888.6	12.1	90.9	
$\nu_{21}+\nu_{29}$	2877 Sh VW	2877.2	10.3	76.7	
$\nu_2+\nu_{29}$	2869 VW	2871.1	9.8	114.2	
$\nu_4+\nu_{24}$	2866 Sh VW	2865.6	12.8	148.7	
$\nu_1+\nu_{18}$, $\nu_{23}+\nu_{24}$, $\nu_3+\nu_{29}$	2851 VW	2854.0	16.6	267.8	
	2846 Sh VW	2845.1	13.8	203.7	
$\nu_2+\nu_{18}$, $\nu_{23}+\nu_{25}$		2822.2	6.0	38.9	
	2820 VW	2820.1	9.0	118.8	
$\nu_3+\nu_{18}$	2810 VW	2811.3	6.6	52.7	
	2806 Sh VW	2808.8	12.1	98.9	
	2790 Sh VW	2789.1	15.8	24.7	
		2742.1	3.8	2.0	
		2739.2	3.8	3.1	
	2737 VW	2736.4	4.6	4.0	
		2732.6	6.5	4.3	
		2724.9	11.8	5.3	
	2694 VW	2696.8	20.7	43.9	
$2\nu_5$	2678 VW	2678.9	10.6	39.9	
$\nu_3+\nu_{19}$		2670.1	11.7	12.4	
	2664 VW	2663.3	11.9	28.6	
$\nu_5+\nu_{24}$	2655 Sh VW	2655.1	14.2	9.4	
	2641 Sh VW	2640.8	13.6	11.9	
$\nu_{14}+\nu_{22}$	2632 Sh VW	2632.7	9.5	9.8	
$2\nu_{24}$, $\nu_5+\nu_{25}$	2627 VW	2627.2	6.5	35.3	
$\nu_1+\nu_{11}$	2614 VW	2614.3	11.9	71.0	
$\nu_2+\nu_{11}$	2589 VW	2588.4	9.7	46.1	
$\nu_4+\nu_6$, $\nu_{23}+\nu_{26}$	2563 Sh VW	2561.5	16.7	63.0	
$\nu_1+\nu_{30}$, $\nu_6+\nu_{23}$	2549 VW	2549.7	11.0	385.8	
$\nu_{21}+\nu_{30}$	2535 Sh VW	2535.8	16.2	54.5	
$\nu_7+\nu_{23}$	2493 VW	2502.3	41.0	69.6	
	2446 VW	2441.3	43.4	89.7	
$\nu_4+\nu_{27}$	2391 VW	I			
$\nu_{23}+\nu_{27}$	2381 VW	2383.4	23.1	319.1	
$\nu_4+\nu_9$	2367 W	2368.0	5.5	139.8	
CO_2(g)	2360VW	2360.3	72.5	0.2	
CO_2(g)	2341 W	2342.9	58.8	1196.4	
ν_1	2307 W	2307.9	7.9	414.9	458.1
		2299.7	4.7	43.2	
$\nu_{25}+\nu_{26}$, $\nu_5+\nu_7$, $\nu_{12}+\nu_{23}$	2297 Sh W	2298.1	4.2	128.0	
ν_{21}	2292 W	2292.7	8.0	1654.1	
ν_2	2281 Sh W	2282.4	8.1	1005.7	
ν_{22}	2276 M	2276.3	9.8	3177.1	
ν_3	2266 W	2266.4	6.4	844.0	2041.3
	2260 Sh W	2260.9	18.5	1197.3	
$\nu_7+\nu_{25}$		2245.7	58.4	775.4	
$\nu_8+\nu_{24}$, $\nu_5+\nu_{27}$, $\nu_{10}+\nu_{23}$	2180 VW	2181.6	18.9	85.8	

(*continued on next page*)

Table 1 (*continued*)

Assignment[a]	obsd $\tilde{\nu}$[b]	Fitted band			Sum of C_j[d]
		$\tilde{\nu}_j$[c]	Γ_j[c]	C_j[d]	
$\nu_5+\nu_{28}$, $\nu_5+\nu_{15}$, $\nu_4+\nu_{17}$	2161 Sh VW	2161.3	4.0	3.3	
$\nu_5+\nu_9$	2154 VW	2155.7	5.5	14.0	
$\nu_{24}+\nu_{27}$	2150 Sh VW	2152.9	5.7	13.5	
$\nu_8+\nu_{25}$		2148.2	7.8	10.0	
$\nu_4+\nu_{29}$, $\nu_1-\nu_{20}$	2138 VW	2139.7	7.1	19.3	
$\nu_{24}+\nu_{28}$		2136.6	6.5	13.7	
$\nu_9+\nu_{24}$	2129 VW	2129.7	6.6	20.0	
$\nu_{25}+\nu_{27}$, $\nu_{23}+\nu_{29}$	2126 Sh VW	2125.4	6.7	10.5	
$\nu_{25}+\nu_{28}$		2100.8	3.1	2.7	
$\nu_3-\nu_{20}$, $\nu_9+\nu_{25}$	2098 Sh VW	2099.0	3.1	3.0	
$\nu_4+\nu_{18}$	2091 VW	2091.8	6.6	63.8	
$\nu_5+\nu_{16}$	2086 Sh VW	2088.9	10.8	24.9	
$\nu_{21}-\nu_{30}$	2058 VW	I			
$\nu_{12}+\nu_{25}$	2048 Sh VW	2048.1	30.6	4.1	
$\nu_6+\nu_{26}$	2031 Sh VW	2032.7	10.4	11.9	
$\nu_3-\nu_{30}$, $2\nu_{26}$	2025 VW	2024.9	17.0	58.7	
$\nu_1-\nu_{11}$	2001 VW	I			
$\nu_5+\nu_{10}$	1981 VW	1982.4	7.6	44.7	
$\nu_2-\nu_{11}$, $\nu_7+\nu_{26}$	1977 Sh VW	1978.5	8.5	19.5	
$\nu_6+\nu_7$	1970 VW	1971.0	9.1	27.9	
$\nu_3-\nu_{11}$, $\nu_{13}+\nu_{25}$	1961 VW	1961.1	9.5	29.2	
$\nu_{10}+\nu_{24}$, $\nu_{21}+\nu_{14}$, $\nu_5+\nu_{29}$, $\nu_5+\nu_{17}$, $\nu_4+\nu_{19}$	1954 Sh VW	1953.9	10.5	18.1	
	1944 VW	1944.7	8.1	15.5	
$\nu_{10}+\nu_{25}$, $\nu_5+\nu_{29}$		1929.2	5.7	4.6	
$2\nu_7$	1917 VW	1917.2	9.9	53.6	
$\nu_1-\nu_{19}$	1903 Sh VW	1904.4	6.1	13.5	
$\nu_{14}+\nu_{23}$, $\nu_{24}+\nu_{29}$	1900 VW	1900.2	5.9	24.8	
	1893 VW	1893.1	7.2	13.4	
$\nu_5+\nu_{18}$, $\nu_8+\nu_{26}$	1888 Sh VW	1888.0	8.3	12.8	
$\nu_6+\nu_8$, $\nu_2-\nu_{19}$	1878 VW	1879.0	9.6	22.2	
$\nu_3-\nu_{19}$	1864 VW	1864.8	5.1	23.6	
$\nu_{26}+\nu_{27}$	1861 Sh VW	1861.0	8.9	20.2	
$\nu_{11}+\nu_{23}$	1848 W	1848.1	4.6	150.4	
		1845.7	3.9	14.2	
$\nu_{26}+\nu_{28}$	1840 VW	1840.0	6.4	85.7	
$\nu_2+\nu_9$, $\nu_6+\nu_{28}$	1832 Sh VW	1831.9	13.6	17.8	
$\nu_7+\nu_8$	1822 VW	1822.6	4.9	21.3	
$\nu_7+\nu_{15}$, $\nu_{23}+\nu_{30}$, $\nu_{12}+\nu_{26}$, $\nu_7+\nu_{28}$	1781 VW	1783.1	11.3	10.3	
$\nu_7+\nu_9$	1773 VW	1773.3	5.2	27.7	
$\nu_6+\nu_{16}$		1753.7	0.9	0.2	
$\nu_3-\nu_{18}$		1725.9	20.1	40.8	
$\nu_8+\nu_{27}$, $\nu_{21}-\nu_{29}$	1707 VW	1707.8	9.6	35.3	
$\nu_8+\nu_{15}$, $\nu_{22}-\nu_{29}$	1687 Sh VW	1687.2	5.9	62.6	
$2\nu_{27}$, $\nu_8+\nu_9$, $\nu_8+\nu_{28}$	1683 W	1683.5	5.4	122.1	
$\nu_3-\nu_{29}$		1681.5	7.5	142.6	
$\nu_1-\nu_{10}$, $\nu_{10}+\nu_{26}$	1664 Sh W	1665.3	7.7	124.5	
$\nu_9+\nu_{27}$, $\nu_{27}+\nu_{28}$, $\nu_2+\nu_{10}$	1659 W	1659.8	6.4	107.2	
$\nu_3-\nu_{17}$	1655 Sh W	1656.5	6.0	76.0	
$\nu_5+\nu_{11}$	1647 W	1648.0	7.0	90.5	
$\nu_9+\nu_{28}$, $\nu_2-\nu_{10}$	1636 Sh W	1640.0	8.2	76.9	
$2\nu_9$, $\nu_6+\nu_{17}$	1632 W	1632.2	9.8	493.5	
$\nu_8+\nu_{16}$, $\nu_{26}+\nu_{29}$	1611 Sh W	I			
$\nu_6+\nu_{29}$, $\nu_{12}+\nu_{27}$, $\nu_7+\nu_{10}$	1600 W	1601.0	6.7	801.3	
		1597.5	5.7	337.0	
$\nu_9+\nu_{16}$, $\nu_6+\nu_{18}$	1557 Sh M	1557.5	8.3	2212.5	
ν_4	1550 M	1551.3	5.3	3188.4	
$\nu_7+\nu_{29}$	1548 Sh M	1548.4	3.5	845.1	
ν_{23}	1539 S	1539.7	5.0	16442.5	
$\nu_3-\nu_{16}$	1527 Sh M	1527.8	5.5	601.6	
$\nu_8+\nu_{10}$, $\nu_5+\nu_{20}$	1509 W	1509.1	6.5	759.4	

(*continued on next page*)

Table 1 (*continued*)

Assignment[a]	obsd $\tilde{\nu}$[b]	Fitted band			Sum of C_j[d]
		$\tilde{\nu}_j$[c]	Γ_j[c]	C_j[d]	
$\nu_7+\nu_{18}$, $\nu_{12}+\nu_6$, $\nu_{13}+\nu_{15}$		1503.2	7.2	200.2	
$\nu_1-\nu_{27}$, $\nu_{10}+\nu_{15}$, $\nu_2-\nu_9$	1466 Sh W	I			
$\nu_2-\nu_{15}$, $\nu_{22}-\nu_{28}$,$\nu_{10}+\nu_{28}$, $\nu_2-\nu_{28}$, $\nu_9+\nu_{10}$	1460 W	I			
$\nu_{27}+\nu_{29}$, $\nu_9+\nu_{17}$	1429 W	1430.6	12.8	339.1	
$\nu_3-\nu_8$, $\nu_9+\nu_{29}$	1403 Sh W	1402.8	5.4	144.5	
	1394 W	1394.6	5.7	512.6	
	1390 W	1390.1	7.1	645.1	
$\nu_{15}+\nu_{18}$, $\nu_7+\nu_{19}$		1362.2	4.1	629.5	
$2\nu_{13}$, $\nu_9+\nu_{18}$	1359 M	1359.5	3.6	731.7	
$\nu_{16}+\nu_{17}$	1356 Sh M	1357.0	3.6	576.8	
		1354.0	3.6	305.8	30691.7
ν_5	1340 S	1340.9	3.5	17314.7	
		1338.9	5.1	6862.2	
	1334 Sh M	1333.4	16.2	6209.0	
ν_{24}	1314 M	1314.2	4.6	5285.9	5836.5
	1307 Sh M	1307.2	5.9	550.6	
		1289.5	5.2	223.4	1290.4
ν_{25}	1285 M	1286.4	5.5	491.5	
		1283.5	6.3	575.5	
	1277 W	1276.7	5.9	624.8	
$\nu_8+\nu_{19}$, $\nu_{13}+\nu_{29}$, $\nu_2-\nu_2$	1268 Sh W	1264.4	9.9	135.0	
$\nu_7+\nu_{11}$, $\nu_2-\nu_{26}$	1261 Sh W	I			
$\nu_{13}+\nu_{18}$	1223 Sh W	1223.3	3.1	45.1	
$\nu_9+\nu_{19}$	1221 W	1221.0	2.7	48.2	
	1218 Sh W	1218.6	2.7	32.1	
	1191 W	1191.8	9.5	501.2	
$\nu_{12}+\nu_{19}$	1164 Sh W	1161.5	5.1	85.1	
$\nu_{17}+\nu_{18}$	1158 W	1157.4	6.4	156.3	
$\nu_{11}+\nu_{27}$, $\nu_{16}+\nu_{19}$, $\nu_4-\nu_{19}$	1147 W	1148.1	7.5	112.2	
	1134 VW	I			
	1092 W	I			
$\nu_{27}+\nu_{30}$	1080 W	I			
$\nu_{10}+\nu_{19}$, $\nu_{11}+\nu_{16}$	1050 W	I			
$\nu_{13}+\nu_{14}$	1041 Sh W	1041.3	13.6	446.1	
$\nu_8+\nu_{20}$, $\nu_5-\nu_{11}$	1032 Sh M	I			
ν_{26}	1020 Sh S	1021.6	6.8	8430.3	
ν_6	1013 S	1013.9	6.6	27283.5	
$\nu_{12}+\nu_{30}$, $\nu_2-\nu_{25}$	1000 Sh M	999.1	7.5	954.5	
$\nu_{14}+\nu_{17}$	970 W	I			
$\nu_4-\nu_{29}$	964 Sh W	I			
ν_7	957 M	957.8	1.9	1669.3	3893.6
	955 Sh M	957.0	2.4	820.1	
		954.2	10.1	1404.2	
$\nu_{10}+\nu_{11}$, $\nu_{18}+\nu_{19}$, $\nu_{14}+\nu_{29}$	948 M	948.1	3.8	233.3	
$\nu_{11}+\nu_{17}$	922 W	I			
	898 W	I			
ν_8	864 M	864.9	4.4	915.1	
$\nu_{23}-\nu_{13}$		863.6	37.5	1005.7	
ν_{27}	840 M	840.4	5.3	1138.5	
ν_{28}, ν_{15}	823 Sh M	823.8	1.8	35.0	
ν_9	816 M	816.6	4.8	3955.7	
$\nu_{10}+\nu_{20}$		814.8	26.0	1465.6	
$\nu_{26}-\nu_{30}$, $\nu_{17}+\nu_{20}$	782 W	782.2	19.1	892.9	
	759 W	I			
ν_{16}	741 M	742.4	3.4	644.6	1617.2
		741.3	4.6	972.6	
	703 W	I			
ν_{10}	643 S	643.3	4.3	13295.5	
ν_{17}	613 S	614.0	5.8	5015.3	

(*continued on next page*)

Table 1 (*continued*)

Assignment[a]	obsd $\tilde{\nu}$[b]	Fitted band			Sum of C_j[d]
		$\tilde{\nu}_j$[c]	Γ_j[c]	C_j[d]	
		587.2	2.0	231.3	
ν_{29}	586 M	586.2	2.6	241.7	620.3
		582.3	6.0	147.3	
	562 M	I			
		546.2	4.4	12225.7	
ν_{18}	544 S	544.5	3.5	11846.5	36999.5
		543.0	4.2	12927.3	
$\nu_{25}-\nu_{28}$, $\nu_8-\nu_{19}$		462.7	10.7	580.9	
$\nu_{13}-\nu_{30}$		442.0	20.9	1714.7	
$\nu_6-\nu_{29}$		424.0	17.6	2470.4	
$\nu_{15}-\nu_{19}$	419 M	I			
$\nu_9-\nu_{19}$		413.9	9.1	952.5	
ν_{19}	405 S	405.6	4.5	15087.9	
$\nu_{10}-\nu_{30}$	403 Sh S	404.0	7.3	4781.4	

[a] Herzberg's notation is used to label the vibrations. The assignments are limited to fundamentals, first overtones and active binary combinations (sum and difference).
[b] The unit is cm^{-1}. S indicates strong, M medium, W weak, VW very weak and Sh shoulder.
[c] The unit is cm^{-1}. I indicates the feature was ignored in the fit.
[d] The unit is cm mol^{-1}. Divide by 1×10^5 to convert to the usual unit of km mol^{-1}.

2. Experimental

2.1. Fitting the imaginary molar polarizability spectrum

The imaginary molar polarizability spectrum [12] between 4000 and 400 cm^{-1} was fitted with CDHO bands [3]

$$\mathrm{CDHO}(\tilde{\nu}) = \frac{Y_j \Gamma_j \tilde{\nu}}{(\tilde{\nu}_j^2 - \tilde{\nu}^2)^2 + \Gamma_j^2 \tilde{\nu}^2} \quad (1)$$

using the curve-fitting program SPECFIT [18]. The parameters obtained from SPECFIT are $\tilde{\nu}_j$, the peak wavenumber; Γ_j, the full width at half height; and a

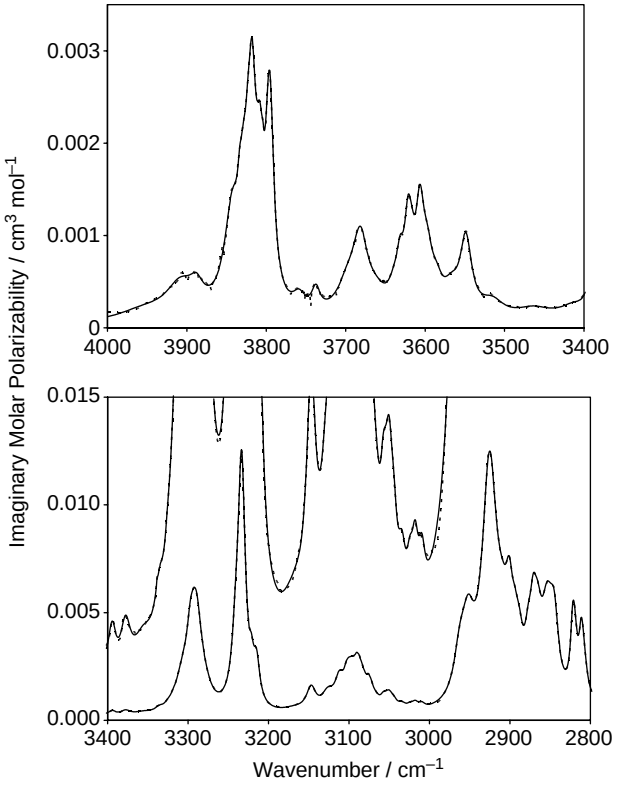

Fig. 1. The experimental (dashed curve) and fitted (solid curve) imaginary molar polarizability spectra of liquid C_6D_5Br at 25 °C between 4000 and 2800 cm^{-1}. The upper spectra in the bottom box are the experimental (dashed curve) and fitted (solid curve) spectra multiplied by 10.

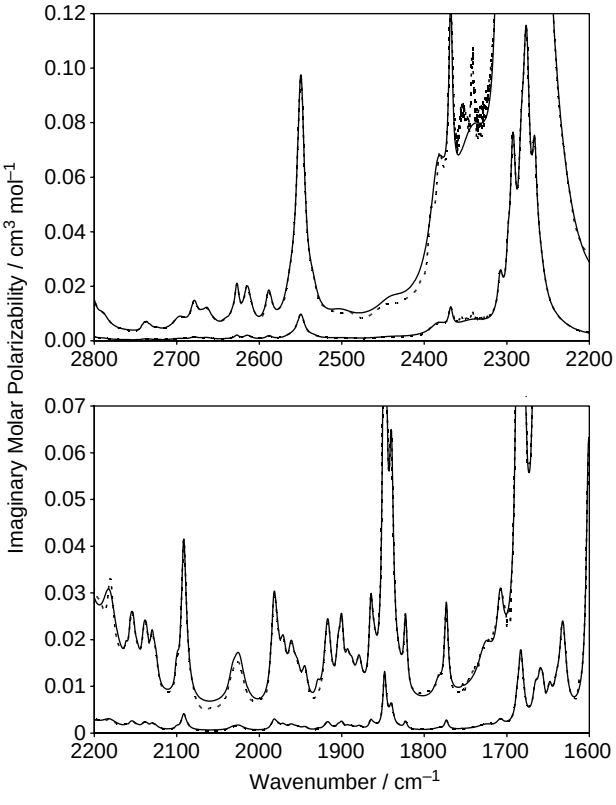

Fig. 2. The experimental (dashed curve) and fitted (solid curve) imaginary molar polarizability spectra of liquid C_6D_5Br at 25 °C between 2800 and 1600 cm^{-1}. The upper spectra in each box are the experimental (dashed curve) and fitted (solid curve) spectra multiplied by 10.

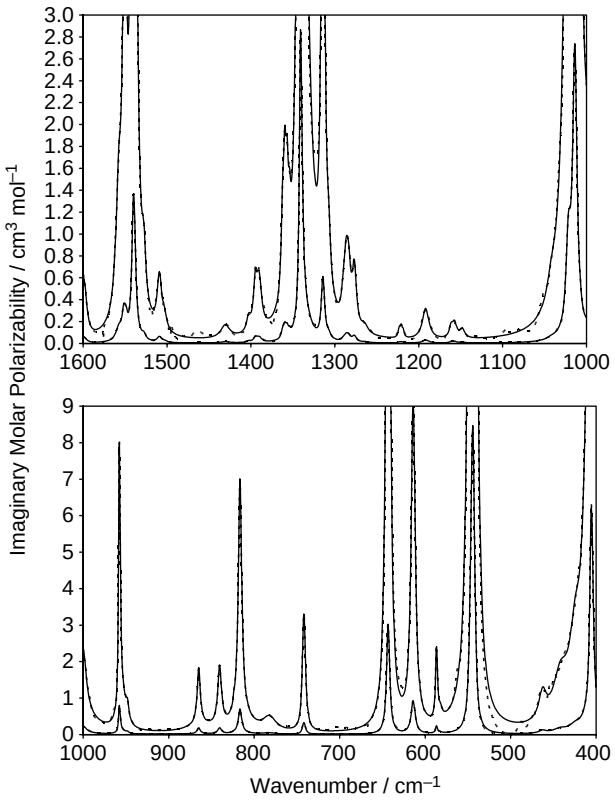

Fig. 3. The experimental (dashed curve) and fitted (solid curve) imaginary molar polarizability spectra of liquid C_6D_5Br at 25 °C between 1600 and 400 cm^{-1}. The upper spectra in each box are the experimental (dashed curve) and fitted (solid curve) spectra multiplied by 10.

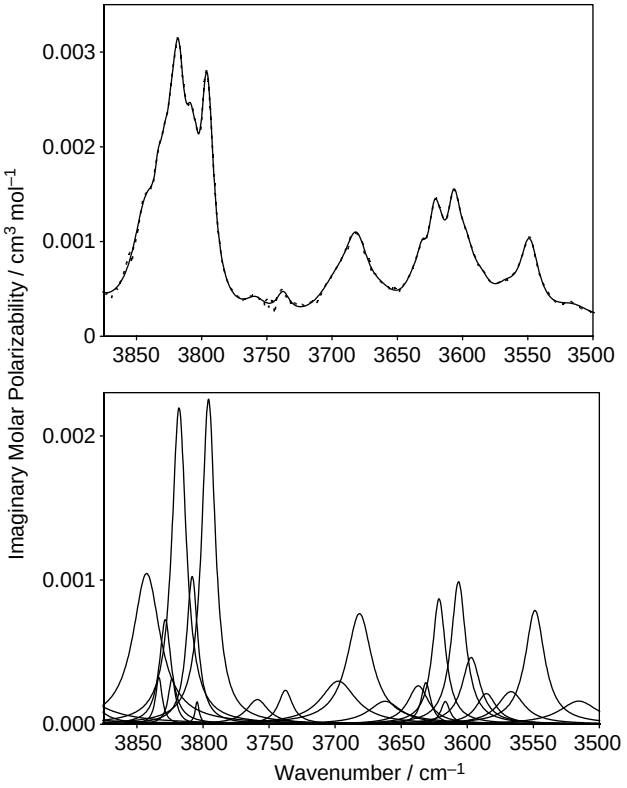

Fig. 4. The experimental (dashed curve) and fitted (solid curve) imaginary molar polarizability spectra (top box) of liquid C_6D_5Br at 25 °C between 3875 and 3500 cm^{-1} and the CDHO bands used to achieve the fit (bottom box).

constant Y_j, that is the peak height in the corresponding band in the $\tilde{\nu}\alpha''_m$ spectrum multiplied by Γ_j [8]. To accelerate the fitting process the bromobenzene-d_5 spectrum was split into four regions, and the regions were fitted separately.

After each region was fitted, the peak parameters for each region were merged together and input into SPECFIT along with the full bromobenzene-d_5 spectrum and the parameters refined. The fit required 231 peaks. In most cases, the bands were needed to fit obvious peaks, shoulders, or asymmetry in the experimental spectrum; in a small number of cases, the bands are simply there to improve the fit, indicating that some peaks may not have a CDHO lineshape. The standard deviation of the fit is 9.4×10^{-3} cm^3 mol^{-1}, the root-mean-square error is 8.9×10^{-3} cm^3 mol^{-1}, and the multiple coefficient of determination [19], R^2, is 0.9995, indicating an excellent fit. An important check, for our purposes, is the agreement of the total areas under both the experimental and fitted spectra. The total area under the fitted spectrum between 4000 and 400 cm^{-1} is 0.63% larger than the total area under the experimental spectrum.

The complete integrated intensity under the $\tilde{\nu}\alpha''_m$ band, C_j,

$$C_j = \int \tilde{\nu}\alpha''_m(\tilde{\nu})d\tilde{\nu} \quad (2)$$

can be obtained from Y_j by $C_j = Y_j\pi/2$. The parameters $\tilde{\nu}_j$, Γ_j, and C_j of the fitted bands are tabulated in Table 1. It is estimated that the C_j values obtained in this way have an uncertainty of about 10% [8].

The quality of the fit is shown in Figs. 1–3, which contain both the experimental and fitted spectra and except for the top box of Fig. 1, all boxes contain the experimental and fitted spectra multiplied by 10. In all cases, the fit is excellent with the difference between the two spectra only visible in a small number of locations.

The quality of the fit and the peaks used to fit the experimental spectrum are illustrated in Figs. 4–6. Shown in these figures are the experimental and fitted imaginary molar polarizability spectra for three regions of varying intensity. In the upper boxes, both the experimental and fitted spectra are given. The peaks used to calculate the fitted spectrum in each region are shown in the bottom boxes. It should be noted that the wings of all the peaks outside the region are included in the fitted spectrum, but for clarity these are not shown. Twenty three peaks are required to fit the region 3875–3500 cm^{-1} (Fig. 4), fifteen peaks are required to fit the region 1960–1830 cm^{-1} (Fig. 5), and eight peaks are required to fit the region 650–500 cm^{-1} (Fig. 6). Most of these are visible in the experimental spectrum as peaks, shoulders, or changes of slope; however, the peaks at 3823, 3804, 3698, 3662, 3637, 1929, 1845, 587, 582, 546, and 543 cm^{-1} were not obvious in the experimental spectrum and are necessary to fit asymmetry

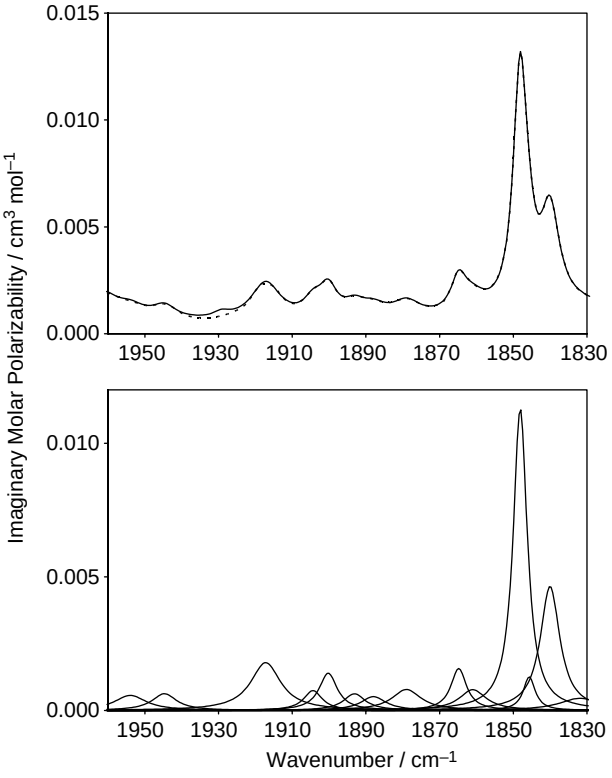

Fig. 5. The experimental (dashed curve) and fitted (solid curve) imaginary molar polarizability spectra (top box) of liquid C_6D_5Br at 25 °C between 1960 and 1830 cm^{-1} and the CDHO bands used to achieve the fit (bottom box).

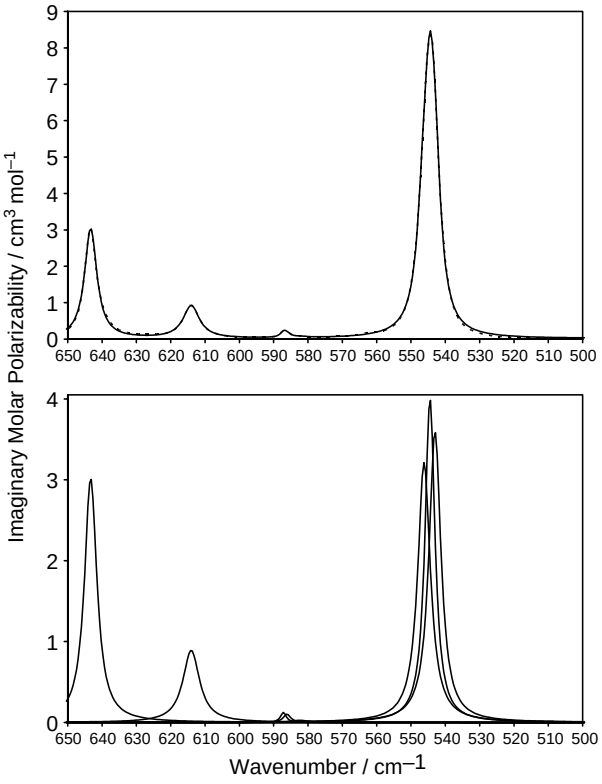

Fig. 6. The experimental (dashed curve) and fitted (solid curve) imaginary molar polarizability spectra (top box) of liquid C_6D_5Br at 25 °C between 650 and 500 cm^{-1} and the CDHO bands used to achieve the fit (bottom box).

of the peaks in the experimental imaginary molar polarizability spectrum. It is impossible, at this stage, to determine if these are real or artifacts of the fitting due to the experimental spectra having a lineshape other than CDHO. However, all of the commonly used lineshapes (such as Gaussian, Lorentzian, or a mixture (additive or product) of the two) are symmetric and would not be able to account for the asymmetry in the experimental lineshape.

3. Discussion

3.1. Assignment of transitions

The vibrational representation for monohalobenzenes is $11A_1+3A_2+6B_1+10B_2$ under the point group C_{2v}, where by convention the x-axis is taken orthogonal to the plane of the molecule. Herzberg's notation [20] is used to number the vibrations throughout this paper. The A_2 vibrations are infrared inactive in the gas-phase and the others are infrared active in the gas-phase. All first overtones and binary sum and difference bands except $A_1\times A_2$ and $B_1\times B_2$ are infrared active.

Included in Table 1 are the assignments of most of the bands used to fit the spectrum. The assignments of the bands are limited to fundamentals, first overtones and active binary sum and difference bands because ternary and larger combinations allow too many possibilities. It is expected that the first overtones and binary sum and difference bands should be the most intense, but it is noted that other overtones and combinations are possible and it is an impossible task to assign them from the current experimental measurements. The fundamentals are those we reported previously [12], which were based on the assignments of Nanney et al. [21]. It should be noted that in the previous work [12], the ν_6 and ν_{26} vibrations were inadvertently interchanged compared to the original work of Nanney et al. [21]. Here, we assign them in the same order as Nanney et al. The assignments of the overtones and combinations are presented as most probable assignments, and when the experimental work is complete on the monosubstituted benzenes some refinement of these assignments may be possible.

The integrated intensity C_j is related to the transition moment, R_j, under the assumption that the hot bands of the fundamental all contribute to the fundamental, by [3,22–24]

$$C_j = \frac{N_A \pi}{3hc_0} g_j \tilde{\nu}_j |R_j|^2 \quad (3)$$

where N_A is Avogadro's number, h is Planck's constant, c_0 is the speed of light in a vacuum, and g_j is the degeneracy of the transition. The integrated intensity can also be related to

Table 2
Integrated intensities, transition moments and dipole derivatives squared with respect to normal coordinates of bromobenzene-d_5 and -h_5

Vibration	Symmetry	Bromobenzene-h_5 (Ref. [1])				Bromobenzene-d_5			
		$\tilde{\nu}_j$(cm^{-1})	C_j (km/mol)	$\|Rj\|$ (D)	μ_j^2(D^{2}A^{-2} u^{-1})	$\tilde{\nu}_j$(cm^{-1})	C_j (km/mol)	$\|Rj\|$ (D)	μ_j^2(D^{2}A^{-2} u^{-1})
1	A_1	3064.4	0.0457	0.0217	0.0854	2307.9	0.00458	0.00791	0.00856
2	A_1	3053.4	0.03488	0.0190	0.0652	2282.4	0.0101	0.0118	0.0188
3	A_1	3040.3	0.0053	0.00744	0.0100	2266.4	0.0204	0.0168	0.0381
4	A_1	1578.4	0.130	0.0366	0.2421	1551.3	0.0319	0.0254	0.0596
5	A_1	1474.1	0.258	0.0718	0.482	1340.9	0.307	0.0849	0.574
6	A_1	1173.6	0.0150	0.0179	0.0281	1013.9	0.273	0.0921	0.510
7	A_1	1067.2	0.127	0.0584	0.238	957.8	0.0389	0.0358	0.0728
8	A_1	1019.1	0.118	0.0590	0.221	864.9	0.00915	0.0183	0.0171
9	A_1	999.6	0.0485	0.0387	0.0906	816.6	0.0396	0.0391	0.0739
10	A_1	672	0.135	0.0653	0.253	643.3	0.1330	0.0807	0.248
11	A_1	312.7	0.0130	0.0247	0.0243	306	NM		
12	A_2	961.6	0.0084	0.0291	0.0157	760	NO		
13	A_2	832.4	0.0084	0.0166	0.0158	680	NO		
14	A_2	409	NO			360	NO		
15	B_1	986.7	0.0275	0.0296	0.0514	823.8	0.000350	0.00366	0.000654
16	B_1	902.4	0.0351	0.0350	0.0656	741.3	0.0162	0.0262	0.0302
17	B_1	736	0.686	0.171	1.28	614	0.0502	0.0507	0.0937
18	B_1	683.9	0.203	0.0966	0.379	544.5	0.370	0.146	0.691
19	B_1	457.6	0.0957	0.0812	0.179	405.6	0.151	0.108	0.282
20	B_1	184.7	0.00853	0.0381	0.0159	170	NM		
21	B_2	3076.9	0.0748	0.0277	0.140	2292.7	0.0165	0.0151	0.0309
22	B_2	3023.8	0.00672	0.00837	0.0126	2276.3	0.0318	0.0210	0.0594
23	B_2	1569.6	0.0584	0.0342	0.109	1539.7	0.164	0.0580	0.307
24	B_2	1442.6	0.113	0.0496	0.211	1314.2	0.0584	0.0374	0.109
25	B_2	1321	0.0154	0.0192	0.0288	1286.4	0.0129	0.0178	0.0241
26	B_2	1263.4	0.0128	0.0179	0.0240	1021.6	0.0843	0.0510	0.158
27	B_2	1157.4	0.0131	0.0189	0.0245	840.4	0.0114	0.0207	0.0213
28	B_2	1069.5	0.0977	0.0537	0.183	823.8	0.000350	0.00366	0.000654
29	B_2	612.4	0.00351	0.0134	0.00656	586.2	0.00620	0.0183	0.0116
30	B_2	246.3	0.000178	0.00477	0.000333	239	NM		

NM, not measured since it is below the cutoff of the spectrometer available for the study; NO, not observed.

the square of the dipole moment derivative with respect to the j th normal coordinate, $\mu_j^2 = |\partial\vec{\mu}/\partial Q_j|^2$, under the double harmonic approximation by [3]

$$C_j = \frac{N_A}{24\pi c_0^2} g_j \mu_j^2 \tag{4}$$

The transition moments and square of the dipole moment derivatives of the fundamentals of bromobenzene-d_5 are given in Table 2 along with those previously reported [11] for bromobenzene-h_5. The estimated [8] 10% uncertainty in C_j results in an approximately 5% uncertainty in the transition moments and dipole moment derivatives.

Under the double harmonic approximation, the integrated intensities of different isotopomers can be compared by the G-Sum and F-Sum rules [25,26]. In addition to the requirements of the double harmonic approximation, the G- and F-Sum are only applicable if either the molecule does not have a permanent dipole moment or if the summation is over vibrations that belong to a symmetry species that does not involve a rotation of the permanent dipole of the molecule. The F-sum, expressed in terms of the integrated intensity C_j and the vibrational wavenumber $\tilde{\nu}_j$, is

$$\sum \frac{C_j}{\tilde{\nu}_j^2} = \text{constant} \tag{5}$$

For bromobenzene the dipole moment is 1.7 D in the gas phase [27], and thus, technically, the sum rules only apply to the A_1 vibrations (the only symmetry species that does not rotate the permanent dipole). However, as a first approximation we can compare the intensities using the sum rule[1]. For the full list of intensities given in Table 2, Eq. (5) equates to 0.361 cm^3 mol^{-1} for bromobenzene-h_5 and 0.346 cm^3 mol^{-1} for bromobenzene-d_5, a 4% difference. Thus, we can conclude that overall the assignments of the intensities for the two isotopomers are consistent.

To further refine the analysis, Eq. (5) can be applied to the individual symmetry species. For the A_1 vibrations, Eq. (5) equates to 0.090 cm^3 mol^{-1} for bromobenzene-h_5 and 0.089 cm^3 mol^{-1} for bromobenzene-d_5, less than 1%

[1] A nonzero dipole moment necessitates the inclusion of the rotational motion as well as knowledge of the force constants [25]. At this time, the force constants are not known and this is the only option available. After the liquid force field is determined as described in the summary, further refinement of this may be possible.

difference. The A_2 vibrations are infrared inactive in the gas-phase and are weak for both isotopomers in the liquid-phase. Eq. (5) equates to 0.248 and 0.233 $cm^3\,mol^{-1}$ for bromobenzene-h_5 and -d_5, respectively, for the B_1 vibrations, a 6% difference. The B_2 vibrations give sums of 0.021 and 0.024 $cm^3\,mol^{-1}$ for bromobenzene-h_5 and -d_5, respectively, a 12% difference. This excellent agreement between the F-sums for the different symmetry species gives us confidence that the integrated intensities are accurate to approximately 10% as was suggested earlier [8].

Work is presently underway in this laboratory to convert the dipole moment derivatives with respect to normal coordinates, already published for three isotopomers of benzene (benzene-h_6 [7], benzene-d_6 [8], benzene-d [9]), to dipole moment derivatives with respect to symmetry and internal coordinates. Once that work is completed, a similar analysis will be carried out for the two bromobenzene isotopomers and the other benzene compounds that are part of this project. This combined with similar studies on the gas-phase spectra will enable the comparison of the dipole moment derivatives for the different benzene compounds and provide insight into how the intermolecular interactions in these liquids affect the charge distribution of the benzene ring and how this in turn affects the vibrational intensities.

4. Summary

The first detailed vibrational assignment of liquid bromobenzene-d_5 is reported, in that the assignment of the overtones and binary combinations are attempted for the first time. The imaginary molar polarizability spectrum, $\alpha''_m(\tilde{\nu})$, was fitted with 231 CDHO bands and the integrated intensity, C_j, calculated analytically from the fitted parameters for each band.

In a future paper, the bromobenzene and bromobenzene-d_5 intensities and wavenumbers will be used to calculate the liquid phase force field and eigenvectors. The intensities will then be related to the dipole moment derivatives with respect to the symmetry and internal coordinates and thus, facilitate a more complete comparison among the mono-substituted benzenes.

Acknowledgement

C.D.K. and J.K.P. thank the Natural Sciences and Engineering Research Council of Canada for funding in support of this work.

References

[1] E.B. Wilson Jr., Phys. Rev. 45 (1934) 706.
[2] J.E. Bertie, S.L. Zhang, C.D. Keefe, Vib. Spectrosc. 8 (1995) 215.
[3] J.E. Bertie, S.L. Zhang, C.D. Keefe, J. Mol. Struct. 324 (1994) 157.
[4] C.D. Keefe, J. Mol. Spectrosc. 205 (2001) 261.
[5] J.E. Bertie, C.D. Keefe, R.N. Jones, Can. J. Chem. 69 (1991) 1609.
[6] J.E. Bertie, R.N. Jones, C.D. Keefe, Appl. Spectrosc. 47 (1993) 891.
[7] J.E. Bertie, C.D. Keefe, J. Mol. Struct. 695–696 (2004) 39.
[8] J.E. Bertie, C.D. Keefe, Fresenius J Anal Chem 362 (1998) 91.
[9] J.E. Bertie, Y. Apelblat, C.D. Keefe, J. Mol. Struct. 550–551 (2000) 135.
[10] C.D. Keefe, J. Pittman, Appl. Spectrosc. 52 (1998) 1062.
[11] C.D. Keefe, L.A. Donovan, S.D. Fleet, J. Phys. Chem. A 103 (1999) 6420.
[12] C.D. Keefe, L.A. Donovan, J. Mol. Struct. 597 (2001) 259.
[13] C.D. Keefe, S. MacInnis, T. Burchell, J. Mol. Struct. 610 (2002) 253.
[14] C.D. Keefe, E. Brand, J. Mol. Struct. 691 (2004) 181.
[15] C.D. Keefe, J. Barrett, L.L. Jessome, J. Mol. Struct. 734 (2004) 67.
[16] J.E. Bertie, R.N. Jones, Y. Apelblat, C.D. Keefe, Appl. Spectrosc. 48 (1994) 127.
[17] C.D. Keefe, J.K. Pearson, A. MacDonald, J. Mol. Struct. 655 (2003) 69.
[18] C.D. Keefe, J. Mol. Struct. 641 (2002) 165.
[19] J. McClave, F. Dietrich, T. Sincich, Statistics, seventh ed., Prentice-Hall, Upper Saddle River, 1997. 553–554.
[20] G. Herzberg, Molecular Spectra and Molecular Structure. II. Infrared and Raman Spectra of Polyatomic Molecules, D. Van Nostrand Company, Inc., Princeton, 1945.
[21] T.R. Nanney, E.R. Lippincott, J.C. Hamer, Spectrochim. Acta 22 (1966) 7337.
[22] J. Fahrenfort, in: M. Davies (Ed.), Infra-Red Spectroscopy and Molecular Structure: An Outline of the Principles, Elsevier, Amsterdam, 1963.
[23] J.W. Warner, M. Wolfsberg, J. Chem. Phys. 78 (1983) 1722.
[24] M.J. Dignam, Appl. Spectrosc. Rev. 21 (1988) 99.
[25] B. Crawford Jr., J. Chem. Phys. 20 (1952) 977.
[26] J.C. Decius, J. Chem. Phys. 20 (1952) 1039.
[27] D.R. Lide (Ed.),79th ed. CRC Handbook of Chemistry and Physics (Electronic Version), Chemical Rubber Company, 1999.